PSFC/JA-10-26

28 GHz Gyrotron ECRH on LDX

P. P. Woskov, J. Kesner, P. C. Michael , D. T. Garnier*, and
M. E. Mauel*

* Columbia University, New York, NY 10027, USA

July 2010

Plasma Science and Fusion Center
Massachusetts Institute of Technology
Cambridge MA 02139 USA

This work was supported by the U.S. Department of Energy, Grant No. DE-FG02-98ER54458. Reproduction, translation, publication, use and disposal, in whole or in part, by or for the United States government is permitted.

28 GHz Gyrotron ECRH on LDX

P. P. Woskov, J. Kesner, P. C. Michael
Plasma Science and Fusion Center, MIT, Cambridge, MA 02139, USA

D. T. Garnier, M. E. Mauel
Department of Applied Physics, Columbia University, New York, NY 10027, USA

Abstract- A 10 kW, CW, 28 GHz gyrotron has been implemented on LDX to increase the plasma density and to more fully explore the potential of high beta plasma stability in a dipole magnetic configuration. This added power represents about a 60% increase in ECRH to a new total of 26.9 kW with sources at 2.45, 6.4, and 10.5 GHz. The 1 Tesla resonances in LDX form small rings encompassing the entire plasma cross-section above and below the floating coil (F-coil) near the dipole axial region. A 32.5 mm diameter TE_{01} waveguide with a partial Vlasov step cut launches a diverging beam from above the F-coil that depends on internal wall reflections for plasma coupling. Initial gyrotron only plasmas exhibit steep natural profiles with fewer hot electrons than with the other sources. The background scattered radiation suggests that only about half the power is being absorbed with the present launcher.

Key Words: magnetic dipole plasma, LDX, electron cyclotron heating, gyrotron, fusion

Introduction

The levitated dipole experiment (LDX) is investigating a magnetic dipole field configuration similar to planetary magnetospheres as an alterative confinement concept for fusion plasmas. Recent experiments have confirmed that stationary, highly peaked plasma density profiles (> 50 core to edge) are formed by the conservation of the product of plasma density and differential flux tube volume ($V = \oint dl/B$). These natural peaked profiles are maintained by ambient plasma turbulence [1], contrary to experience with plasmas inside a set of coils where turbulence acts to flatten profiles. This new laboratory achievement has obvious potential implications for fusion confinement [2] that could lead to advanced fuel cycle reactors [3].

LDX uses a 1.1 MA, 34 cm mean radius, 560 kg superconducting coil (F-coil) that is freely floated inside a large 5 m diameter vacuum chamber by a 280 kA levitating coil for over 2 hours between cryogenic recoolings [4]. Plasmas are started and sustained by electron cyclotron resonance heating (ECRH) on closed flux surfaces encircling the F-coil that cross the outer midplane radius between 68 and 171 cm. The magnetic field strength varies from 0.007 to 3.2 Tesla around the F-coil on these flux surfaces making possible ECRH over a wide range of frequencies.

A 10 kW, 28 GHz gyrotron has been added to the existing complement of four other ECRH sources consisting of: two 2.45 GHz magnetrons at 2.5 and 1.9 kW, a 2.5 kW, 6.4 GHz klystron, and a 10 kW, 10.5 GHz klystron. The gyrotron increases the total ECRH power on LDX by 60% from 16.9 to 26.9 kW. This continues the build up of the LDX facility from initial operation with just two ECRH sources [5] and brings to realization an early goal of LDX to use 28 GHz ECRH with other sources to investigate high beta plasmas, pressure profile control, plasma stability and confinement. The added

gyrotron power will make possible higher plasma densities with a resonant surface close to the inside dipole "hole" where flux surfaces are compressed together enabling uniform heating across the plasma cross section with a stable source pressure profile less steep than the adiabatic condition $\delta\left(pV^{\gamma}\right)=0$, where p is pressure and γ=5/3 [6].

Gyrotron Installation

The gyrotron source is a commercial turn key system, CPI HeatWave Model VIA-301. The gyrotron resonator operates in the second harmonic circular TE_{02} mode, which is converted to the TE_{01} mode for transmission to LDX. The gyrotron tube and permanent magnet are located on the LDX midplane balcony about 7 meters from the dipole axis and oriented with the resonator field parallel to the vertical LDX stray field of about 2 Gauss. There are no apparent complications due to stray field interaction between the gyrotron and LDX.

The transmission line is a 32.5 mm internal diameter copper line approximately 5 m long with one internally corrugated 90° bend above the gyrotron to direct the vertical upward gyrotron output horizontally toward LDX. The gyrotron beam enters the LDX vacuum chamber through a port in the upper domed region at a radius of about 2 m ($r \approx 2$ m) from the dipole axis and about 1 m above ($z \approx 1$ m) the midplane. The vacuum window is a 44 mm diameter, one wavelength thick, fused quartz disk that is edge water cooled. Arc detectors are located at both the LDX and gyrotron windows.

The waveguide continues inside the vacuum chamber a short distance and terminates in a Vlasov step cut [7]. There is no parabolic reflector and the step cut is only 30 mm long rather than the 74 mm specified for this diameter waveguide and mode. Consequently, the launched power diverges rapidly with little directivity toward the plasma with a range of vertical and horizontal polarization. Coupling to the plasma relies on multiple reflections from the vacuum chamber walls as is the case for the other ECRH sources [5]. The metal chamber walls and F-coil reflect microwaves and do not absorb significant ECRH power. Consequently, the added gyrotron power has not reduced levitation time below typical 2 hour flights.

Plasma Absorption

Even though the launched gyrotron power has little directivity, it is worthwhile to consider first pass absorption to gain insight into 28 GHz ECRH in LDX. Figure 1 shows a vertical cross section of LDX through the F-coil diameter. The small dashed contours encircling the F-coil define the inner and outer closed flux surfaces. The larger dashed contour crossing the dipole axis defines the 1 Tesla field surface that would be resonant at 28 GHz in a cold plasma. The first pass incident power from the center of the launch aperture at r = 190 cm and z = 106 cm is illustrated by rays A and B. These rays represent limiting cases for propagation with respect to magnetic field with ray A near perpendicular and ray B near parallel in the absorption region.

The plasma is confined between the inner and outer flux surfaces with a highly peaked natural profile [1] as illustrated in Figure 2. Here we are assuming the plasma is peaked on the flux contour crossing the midplane at r = 75 cm with a $1/r^4$ density dependence and a $1/r^3$ temperature dependence, which would be consistent with expected magnetic dipole pressure profiles of about $1/r^7$ [1,6].

ECRH would primarily act on the hot tail of the electron distribution function which is observed in LDX with x-ray and electron cyclotron emission diagnostics [8]. Using the EC absorption coefficient expression give by Equations 1 and 2 in [9], absorption contours for x-mode are shown in Figure 1 for the first pass rays A and B assuming a conservative hot electron temperature peak of 10 keV. The contours shown are all due to the fundamental EC resonance. Harmonic absorption is not significant for the hot electron parameters modeled here. Note that the quasi-perpendicular incidence ray A is from the high field side of the plasma, circumventing the x-mode right hand cutoff.

It is readily apparent that the 28 GHz absorption regions in LDX form localized rings above (shown) and below (not shown) the F-Coil that encompass the entire plasma profile between the inner and outer closed flux surfaces. For a peak hot electron density of 10^{11} cm^{-3} at 10 keV the absolute value of the electron cyclotron wave (ECW) x- and o-mode absorption coefficients for rays A and B is plotted in the top graph of Figure 3. For quasi-perpendicular propagation x-mode absorption is stronger while for quasi-parallel incidence both x- and o-mode absorption is similar.

Integrating the absorption coefficient along the propagation of each ray the absorption fraction, *A*, can be calculated by the formula:

$$A = 1 - e^{-\tau}, \qquad \tau = \int \alpha ds \tag{1}$$

where α is the absorption coefficient and *s* is the path along the ray. The absorption fraction for rays A and B is plotted in the lower graph of Figure 3 showing that even with a low peak hot electron density of 10^{11} cm^{-3} over 90% and 70% of the quasi-perpendicular and quasi-parallel incident power, respectively, can be absorbed on one pass through the resonance zone. The absorptions zones however are small relative to the vacuum chamber distributed power and the incident polarization does not exactly match, requiring many wall reflections for complete power absorption.

Initial Results

In the first plasma campaign with the gyrotron, 28 GHz power did add plasma density but generated fewer hot electrons. Figure 4 shows data for a plasma shot with gyrotron only ECRH. The top plot of interferometer density traces shows decreasing plasma density in going from the central chord (ch.1) to an outer chord (ch.3) as indicative of a steep plasma profile [1]. Not shown, the x-ray and ECE signals are down about a factor of 4 to 5 relative to plasmas started and sustained with the other ECRH sources. The smaller hot electron population may be related to gyrotron ECRH being nearer the throat of the dipole where hot electron trapping may be diminished. This will be investigated in future campaigns.

There is evidence that not all the 28 GHz power is being absorbed with the present launch configuration. The middle plot in Figure 4 shows the scattered vacuum chamber radiation being picked up by a Schottky diode detector in a port about 1.2 m below and behind the 28 GHz waveguide launch aperture. The signal from two gyrotron pulses is shown: one with plasma and one without. The mean signal level with plasma is only decreased about 50% from the reference pulse with no plasma, suggesting that the gyrotron power coupling to the plasma absorption regions is not optimized.

Another feature evident in the scattered background is the significant peaks during the 3 second power ramp up and down (a limit of the commercial system). The 28 GHz forward power signals plotted in the bottom graph do not show these peaks. Forward power is picked up by a 28 GHz TE_{02} directional coupler at the gyrotron that is only sensitive to this mode and frequency. The Schottky diode on LDX has no such limitation and is sensitive to other frequencies and modes. Consequently, the peaks in the background signal are due to other gyrotron modes that turn on and off during gyrotron ramping on the desired mode. In particular, the fundamental 15 GHz TE_{01} mode is expected to be present and likely the strongest spurious peak. How this impacts the plasma parameters will be another topic of future study.

Concluding Remarks

The 28 GHz gyrotron has operated well in its first plasma campaign achieving over 70 full power pulses with flat tops lasting 5 seconds or more. It has been used alone and in combination with the other ECRH sources. Insights gained from the first campaign will be used to make future improvements. This will include implementation of a full Vlasov antenna with parabolic mirror to direct more of the gyrotron power at the plasma. Also the higher density plasmas will improve wave propagation for the addition of ICRH, the next planned plasma heating upgrade to LDX.

The magnetic dipole represents unique field geometry for ECW-plasma interaction studies because of the extreme magnetic field range and curvature exposed to ECRH. Future work at LDX will continue to research multi source ECRH in a magnetic dipole for advanced fusion cycles [3] and could also contribute to fundamental ECRH/ECCD physics understanding relevant to other magnetic confinement approaches.

Acknowledgement

R. F. Ellis of the University of Maryland is gratefully acknowledged for making possible the loan of the gyrotron.

References

1. A. Boxer, R. Bergmann, J.L. Ellsworth, D.T. Garnier, J. Kesner, M.E. Mauel, P. Woskov, Nature Physics, **6**, 207-212 (2010)
2. J. Weiland, Nature Physics, **6**, 167-168 (2010)
3. J. Kesner, D.T. Garnier, A. Hansen, M.E. Mauel, L. Bromberg, Nuclear Fusion **44** 193-203 (2004)
4. A. Zhukovsky, P.C. Michael, J.H. Schultz, B.A. Smith, J.V. Minervini, J. Kesner, A. Radovinsky, D. Garnier, M. Mauel, Fusion Eng. and Design, **75-79**, 29 (2005)
5. A.K. Hansen A.C. Boxer, J.L.Ellsworth, D.T. Garnier, I. Karim, J. Kesner, M.E. Mauel, E.E. Ortiz, J. Fusion Energy, **26**, 57-60 (2007)
6. D.T. Garnier, J. Kesner, M.E. Mauel, Radio Frequency Power in Plasmas, S. Bernabei and F. Paoletti, eds., American Institute of Physics, 273-276 (1999)
7. O. Wada and M. Nakajima, EC6 Joint Workshop on ECE and ECRH, Oxford, 369-374 (1987).
8. P. P. Woskov, J. Kesner, D. T. Garnier, M. E. Mauel and S. H. Nogami, LAPD14, Treviso, Italy, Journal of Physics: Conference Series, **227**, 012021, 2010.
9. A. Nassari and M. Heindler, Phys. Fluids, **31**, 95-98 (1988

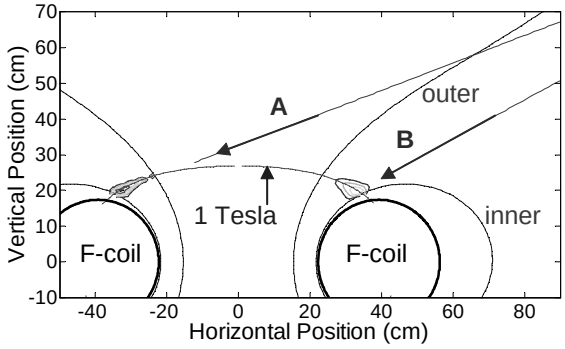

Figure 1. Cross section of LDX F- coil and flux surfaces showing 10 keV EC absorption coefficient contours for 28 GHz incident rays A and B

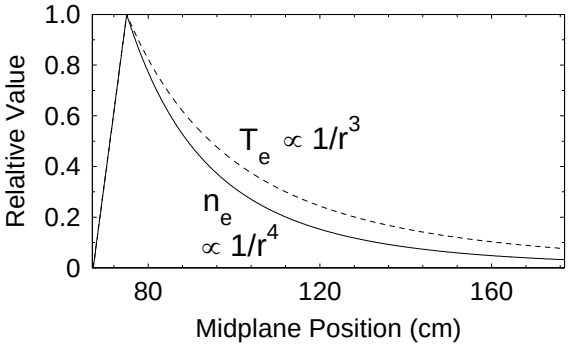

Figure 2. Electron density and temperature profiles used for modeling EC absorption in LDX.

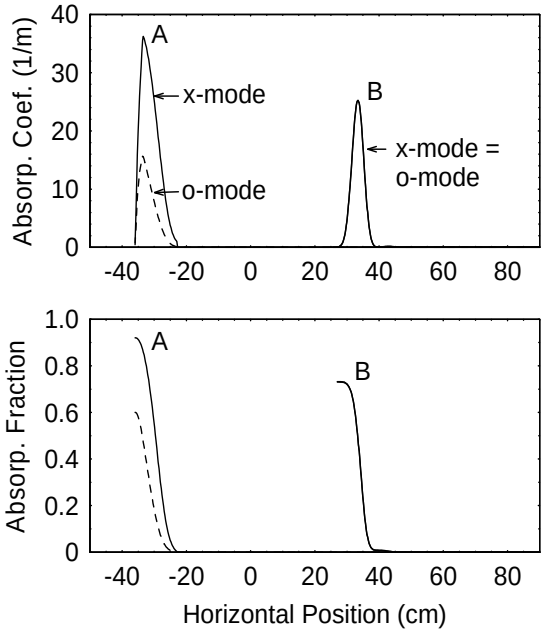

Figure 3. Top: electron cyclotron absorption coefficient for T_e =10 keV and n_e= 10^{11} cm^{-3}, Bottom: absorption fraction for propagation from right.

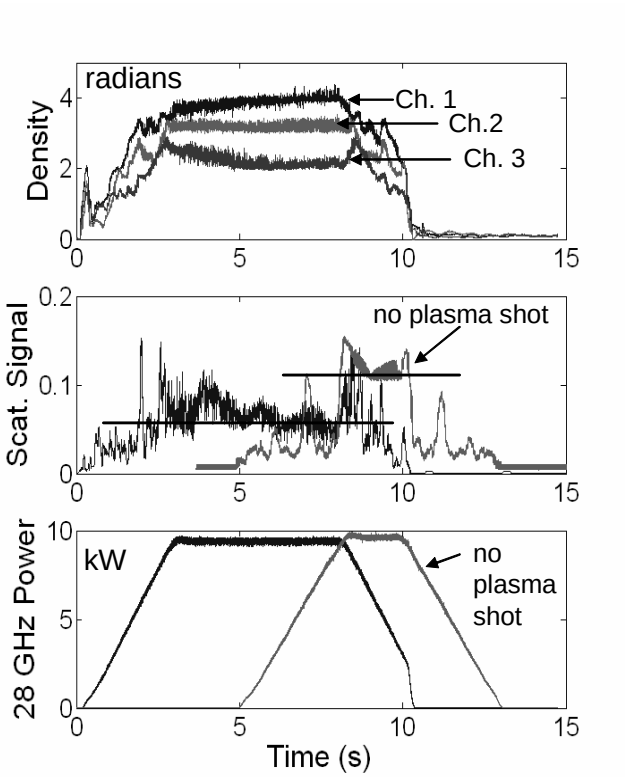

Figure 4. Data for plasma shot #100128016 with gyrotron only ECRH. Top: integrated electron density 60 GHz interferometer traces (peak density mid 10^{11} cm^{-3} range), Middle: microwave background radiation inside the vacuum chamber with plasma and without plasma, Bottom: gyrotron 28 GHz forward